Modeling Dynamic Urban Growth Using Cellular Automata and Geospatial Technique: Case of Casablanca in Morocco

Benchelha, N.,[1*] Bezza, M.,[2] Belbounaguia, N.,[3] Benchelha, S.[1] and Benchelha, M.[1]
[1]Electronic, Automatic Energy and Information Processing Laboratory (EEA &ti), Faculty of TechnicalSciences, B.P 146 Mohammedia 28806, Morocco
E-mail: najat.benchelha@gmail.com, benchelha.said2@gmail.com, benchelha.doc@gmail.com
[2]GAIA Laboratory,Hassan II University of Casablanca, Faculty of Sciences, Ain Chock, Morocco
E-mail: mohamed.bezza@fstm.ac.ma
[3]Geosciences Laboratory,Hassan II University of Casablanca, Faculty of Sciences, Ain Chock, Morocco
E-mail: noureddine.belbounaguia@fstm.ac.ma
Corresponding Author

DOI: https://doi.org/10.52939/ijg.v18i5.2369

Abstract
The rapid urbanisation contribute to the spatial expansion in cities.However, the rapid and unmanaged urban growth, degraded the urban environment. In casablancathe economic engine of Morocco, the rapid urbanization was a result of demographic explosion, rural exodus, and the introduction of new urban projects.Understanding the interdependencies between urban growth patterns, infrastructure, and socioeconomic indicators is a critical step in achieving a sustainable urban development. In order to help Casablanca's sustainable growth, this study used remote sensing data to evaluate past urban land use changes. This study was conducted to examine past urban land cover change on the basis of remote sensing data collected between 1989 and 2019.To forecast the city's expansion for the years 2019e2029, an integrated Cellular Automata urban growth model was used. The research looked into the CA algorithm's capacity to work independently for urban development modeling satellite data from four time periods at equal intervals, as well as population density, distance to the city center, slope, and distance to roadways, are used for this purpose.Between 1989 and 2019, the satellite-based LULC reported an increase of 61.77Km2 (an 88 percent increase). The principle component analysis (PCA) technique was used to analyze geographic variation and found good classification similarity ranging from 87 to 90%. Based on the anticipated LULC, the built-up area will grow to 131.88 km2 in 2019, mostly in the west and southwest. Urbanization will replace and transform other LULC (net loss of 15.348Km2) between 2019 and 2029, followed by plant cover (net loss of 1.608Km2).

1. Introduction

Rapid city economic development and population growth have triggered the uncontrolled expansion of metropolitan areas in the country (Liu et al., 2014 and Seto, 2011), which has a significant impact on the complex socio-economic systems. Therfore, recent recherches (Liao and Dennis Wei, 2014) have focused more on inter relationships, between urbanization and ecological impacts (Mohammadyand Delavar, 2016).

To simulate land use alterations and anticipate their ecological consequences, a large range of models have been used (Navid, 1989). They've also become an important tool for policymakers in urban planning and management (Saadani et al., 2020). At the turn of the twentieth century, the application of a spatial information system (GIS) in urban expansion modeling was important (Batty et al., 1999 and Michalak, 1993), to understand the predictor variables of spatio–temporal changes. For their efficient spatial computational capabilities, regression models (Liao and Dennis Wei, 2014, Hu and Lo, 200, Mom and Ongsomwang, 2016, Tahami et al., 2018 and Tayyebi and Pijanowski, 2014),including artificial neural networks (ANN) (Pijanowski et al., 2002, Mohammady and Delavar, 2016, Pijanowski et al., 2000, Tayyebi et al., 2011, Pourebrahim et al., 2018 and Tian et al., 2016)and agent-basedmodels (ABM)(Hosseinali et al., 2013 and Babakan and Taleai, 2015) are used.

Models ofcellular automata (CA) are typically regarded as the most functional instruments (Li and Yeh, 2002, Shi and Pang, 2000, He et al., 2006, Zhang et al., 2011, Wu and Martinm 2002 and Tobler, 1970). Tobler (1970) suggested the urban CA model in 1970 to replicate Detroit's urban expansion. The Slope Land cover Exclusion Urbanization Transportation Hillshade (SLEUTH) was employed CA algorithmto simulate shifts in land cover in San Francisco (Clarke et al., 1997). Batty and Xie (1994) used the CA model to study urban developments in Baffalo. Wu (2002) created a logistic regression CA model to study Guangzhou's urban growth. He et al.,(2005) used a combination of system dynamics and CA models to predict land use shifts in northern China. Li and Yeh (2004) used data mining and CA to mimic Dongguan's urban expansion. The CA model was used by (Li et al., 2012) to simulate advances in urban land use in the province of Guangdong using the GPU approach. Mustafa et al., (2017) used automata cellular and agent-based techniques to predict urban expansion in Wallonia, Belgium, from 1990 to 2000. Liu et al., (2014) employed the Landscape Expansion Index (LEI) and the CA algorithme to examine the urban growth of cities in the Pearl River Delta. In the recent three decades, research using CA urban growth models has exploded, providing in-depthknowledge into urban growth policies and contributing in the formulation of urban growth strategies to assure a Future urban sustainability (Wu and Martin, 2002). CA models' urban simulation and prediction capabilities have been proved and successfully used all around the world for throughout the previous fifteen years (Chaudhuri and Clarke, 2013).

In this study, we aimed to examine over the past decades the spatio–temporal Land use and cover dynamics (LULC) in order to model urban development for the municipality of Casablanca, Morocco using the CA algorithm. Modelling of urban growth in this area has been the subject of several research studies. For example, Mallouk et al., (2019) developed an urban growth prediction model that is based on the SLEUTH model. The approach entails calibrating the model using data extracted from historical, satellite imagery. Saadani et al., (2020) developed a CA-based Markov Chain (CA-MC) approach to simulate the growth of Moroccan cities. The model combined CA-MC with Landsat images to forecast LULC. The prediction outcome calls for the institution of novel environmental protection measures and the promotion of sustainable growth. Jaad and Abdelghany (2021) studies the urban growth pattern in five major cities one of them citie of casablanca. The study uses a machine learning (ML)-based modeling framework that combines computer vision and remote sensing techniques to produce high-fidelity urban growth predictions. In this analysis, the LULC of four separate years: 1989, 1999, 2009, and 2019 was evaluated. In order to achieve this objective,we also considered other factors and growth parameters, for exemple topography, road proximity, proximity to the city center, areas with growth constraints, as well as demographic statistics. The future projection proved valuable inextrapolating the environmental implications of Casablanca's urbanization, which could help improve sustainability. In addition, we discuss the CA model's accuracy and dependability of the in simulating the urban development of Casablanca, Morocco. Casablanca's urban area has grown in recent decades, thus it appears appropriate to investigate this pattern and determine how it might affect other land use features

2. Study Area

Casablanca is the Moroccan kingdom's economic capital and biggest metropolis, located in the country's center-west on the Atlantic coast (Lat. 33°36′N, Long. 07°36′W) (Figure 1). With an estimated population of 4,270,000 (RGPH1, 2014) for an area of 1,615 km2, it is Morocco's most populous metropolis. Casablanca, Mohammedia, Nouaceur, and Mediouna are the four provinces that make up its territory (Figure 1). The city had significant growth in the last century as a result of its geographical location, which facilitated land and maritime trade.

Urbanization, population increase, and the region's industrial and commercial influence have all contributed to a decline in environmental quality, which has come at the expense of agricultural land.Among the environmental results of urban growth is road traffic congestion and air pollution associated with this traffic. Taking into account and understanding the interaction between transport and urban planning is necessary and essential for planners.

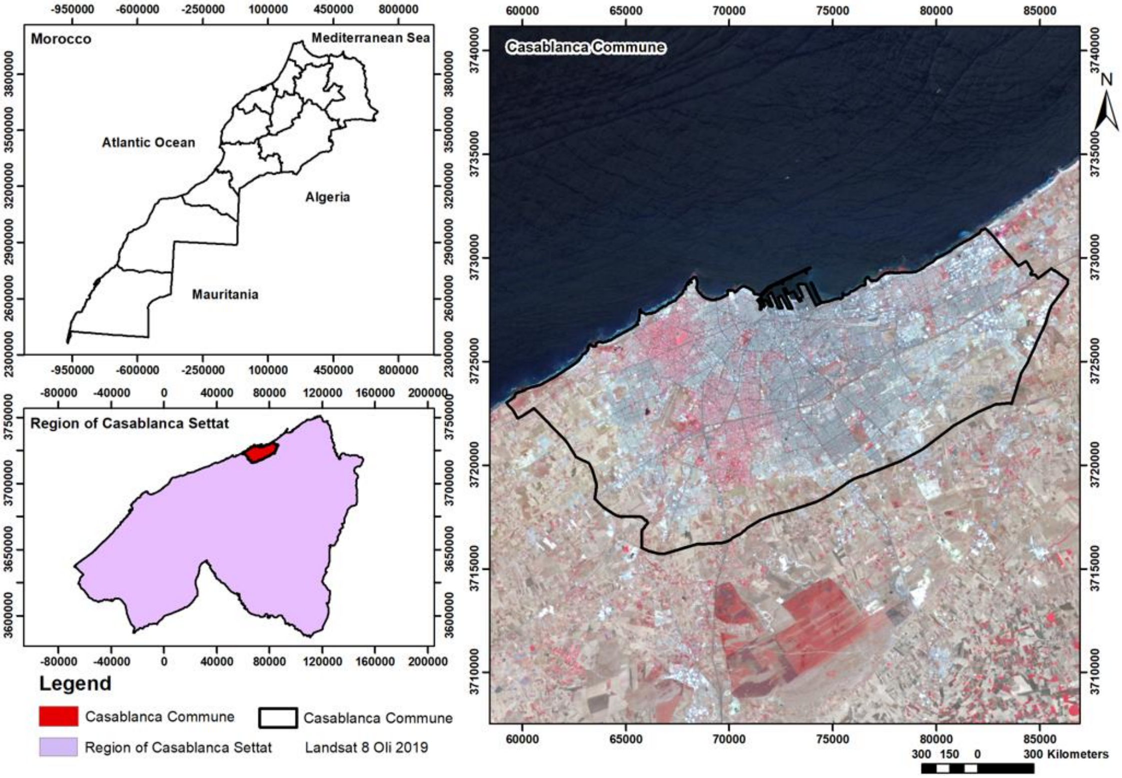

Figure 1: Map of the study area

Casablanca has a temperate climate similar to that of Southern California's coast: in fact, a cold current flows down the Atlantic Ocean's shore, causing morning fogs and cooling the summer heat. The average temperature in Casablanca varies from 13°C in January to 24 °C in August.During winter, temperatures are a little lower in inland areas, but during summer, they are higher. Extreme hot weather is rare thanks to the Atlantic's maritime effect, especially in coastal areas and in comparison to other parts of Morocco.

3. Methods and Data

Nombreuses thematic layers satellite images were selected for this study. Purposes of modelling, many parameters encouraging urban expansion with LULC were generated as raster layers, including population density, road network proximity, slope, and the city center's vicinity (Figure 2). To obtain the best potential threshold values, a model was fine-tuned to maintain the LULC simulation statistically and geographically close to the genuine LULC. For built-up estimates for the years 2029, the trend of the derived threshold values was evaluated.The LULC, road network, and other thematic layers were created in ArcGIS 10.3, while the calibration and future projection were carried out in Python 3.8.

3.1 Thematic Layers

Multi-temporal "LANDSAT" satellite images at 10-year intervals from 1989 to 2019 were downloaded from the USGS website.In order to create the different LULC classes: water, vegetation, buildings and the "other" class, the classification of the images was carried out according to the Maximum Likelihood Supervised Classification Algorithm (Tables 1-2). Four "LANDSAT" multi-temporal satellite images (1989, 1999, 2009 and 2019) were downloaded from the USGS website.These images were preprocessed by stacking the layers (bands 2, 3, 4, 5, 6 and 7). An atmospheric correction is considered an essential step in the pre-processing phase. Landsat images collected along the same satellite path were mosaicked into a single image.

In order to create the different LULC classes: water, vegetation, buildings and the "other" class. Supervised classification was performed on these images using a maximum likelihood algorithm based on training region signatures (Tables 1-2). The purpose of this study was to develop a design for the constructed class of characteristics, which comprises residential areas, institutions, informal settlements, and industries. If there was any type of green cover spaces, it was classified as vegetation.

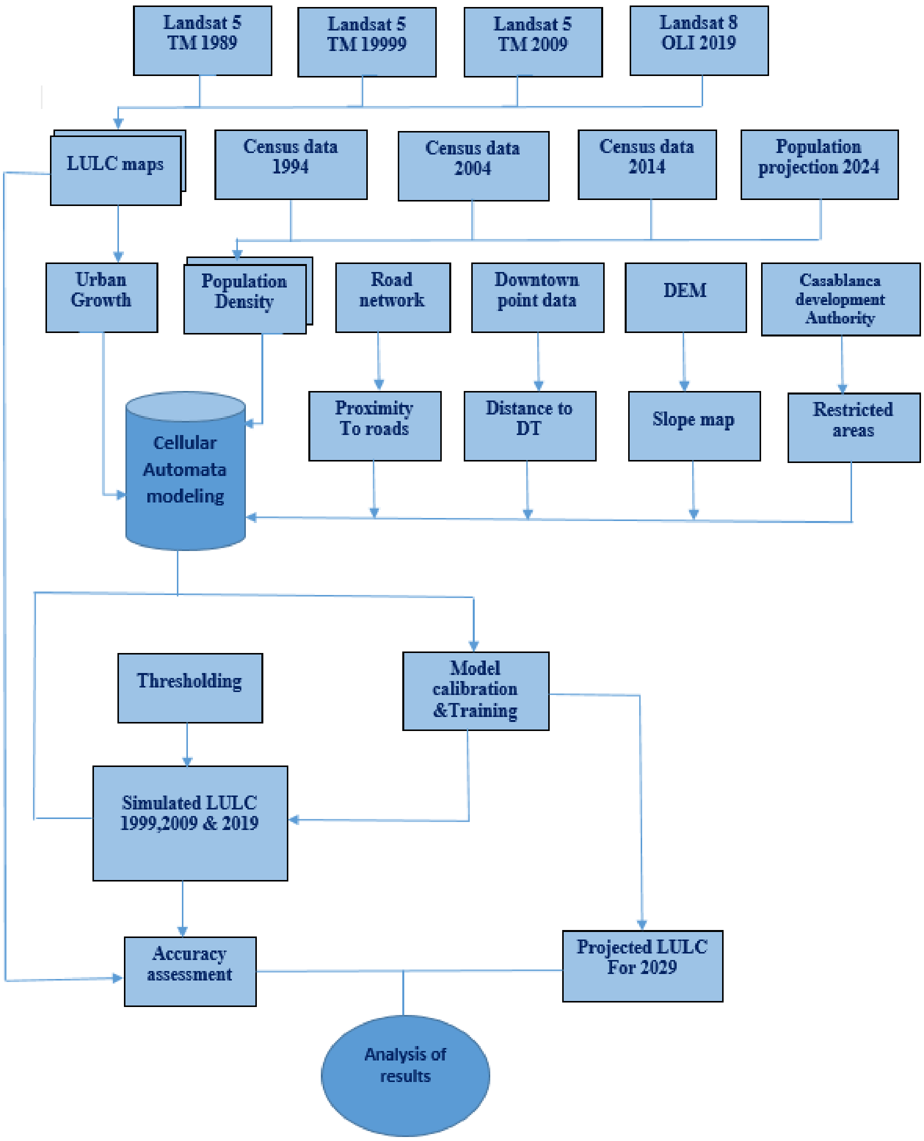

Figure 2: Methodology flow chart of urban CA model

Water zones contained streams, canals and other bodies of water, while the rest was classified as other, mostly agricultural land. The accuracy assessment approach was used to validate the satellite maps categorised by the LULC, utilizing 100 randomly selected points as validation samples. Field checks and Google Earth photos verified these points for images taken between 2009 and 2019.Experts from local government employees, including the regional forest management, the basin agency, and the municipality of Casablanca, as well as ancient maps, were used to analyze the pictures from 1989 and 1999. For each of the observation years (1989, 1999, 2009, and 2019), the average precision was calculated; it varied from 87 to 90%, with a kappa coefficient of 0.74 to 0.82.

The finished LULC maps were used to study LULC transition and urban sprawl from 1989 to 2019, as well as to calibrate the model. For the simulations, the Moroccan censuses (1994-2004-2014) provided the population data, as well as the model's calibration. The population density map for 2024 was utilised for future forecasting purposes. The density of the different areas of Casablanca was determined via the vector layer property. It was then converted into a raster layer of 30 x 30 m to accommodate the geometry of the other contributing layers. The slope maps in all three groups (3, 3–5,> 5) were created using a USGS-provided Digital Elevation Model with a spatial resolution of 30 meters.

Table 1: Details of the analysis's input data

Data type	Details	Date of acquisition
LANDSAT 5 TM	Path : 202 ; Row : 37	1989/08/07
LANDSAT 5 TM	Path : 202 ; Row : 37	1999/07/02
LANDSAT 5 TM	Path : 202 ; Row : 37	2009/06/27
LANDSAT 8 OLI	Path : 202 ; Row : 37	2019/06/23
Digital Elevation Model	ASTER Global Digital Elevation Model V003 (spatial resolution 30m)	2000-03-01
General Population and Housing Census	high commission for morocco plans	1994, 2004, 2014 and 2024

Table 2: Characteristics of the different LULC classes

Feature class	Characteristics	Description
Built-up	Consist of	All man-made structures that are primarily impervious including residential areas, commercial areas, withlow economic relevance
	proximity	Parks, plantations, lakes, ponds, transport networks
	significance	high to moderate population density
Vegetation	Consist of	All green spaces and forests in the urban area and its surroundings, including agricultural land, parks, plantations, protected forests, agriculture
	proximity	Moderate to low built-up structures and water bodies
	significance	Public, private and government preserved area
Water	Consist of	All water bodies
	proximity	Low/high vegetation, open land
	significance	Potable/non-potable water, contaminated, irrigational
Other	Consist of	Toutes les caractéristiques à l'exclusion des constructions, de la végétation et de l'eau
	proximity	Low / high vegetation, built structures
	significance	Belonging to the private domain of the state and or to individuals

The primary road network was derived from a satellite image showing closeness to important roads at intervals of 250 metres by 3 kilometres. Similarly, 12 classes of circular buffer were sampled at 1 km intervals over the city area. To increase the model's capacity to recreate the current growth system, a layer for restriction zones was explored. Pixels gathered in confined areas indicating the forest and land occupied by this binary layer were not produced by the model.

3.2 Modeling Algorithms for CA

The CA models are self-organizing, rule-based, and spatially explicit, making them appropriate for predicting urban land use change (White and Engelen, 2000). As a result, the models CA are increasingly being used in simulations of changing land use and urban growth modeling (Clarke et al., 1997). A script for the CA model has been written to account for all of the elements that lead to urban expansion in Casablanca. As stated in Equation 1, a kernel of size 3*3 kept the test pixel in the middle.

$$A_{ij}^{t} = \begin{bmatrix} a_{i-1j-1}^{(t)} & a_{i-1j}^{(t)} & a_{i-1j+1}^{(t)} \\ a_{ij-1}^{(t)} & a_{ij}^{(t)} & a_{ij+1}^{(t)} \\ a_{i+1j-1}^{(t)} & a_{i+1j}^{(t)} & a_{i+1j+1}^{(t)} \end{bmatrix} \quad \text{3*3neighbourhood}$$

Equation 1

ISSN: 1686-6576 (Printed) | ISSN 2673-0014 (Online) | © Geoinformatics International

The model is essentially based on the current state of the test pixel, the current state of adjacent pixels, and a set of transformation rules (Kumar et al., 2009). It's critical to match layer geometry across all raster layers to ensure that any random pixel (ai, j) represents the same section of the terrain. The dependence of the pixel's future state (t + 1) on the passage rules (Ø) and the normal state has been investigated using Equation (2):

$$a_{i,j}^{t+1} = \emptyset\ (a_{i,j}^{t})$$

Equation 2

The passing rules (φ) were based on a collection of threshold conditional statements that looked like this:

$$\emptyset = f\ (T,B)$$

Eqaution 3

The transition rules appear to be a function of T, a set of threshold values for all the impacted parameters, and B, a set of kernel count values associated with each set of T, according to Equation (3).

$$T= \{T_R,T_C\ ,T_P,T_S\}$$

Equation 4

$$T= \{B_R,B_C\ ,B_P,B_S\}$$

Equation 5

where TR, TC, TP, and TS are the corresponding number of pixels incorporated in the test kernel for each element belonging to T; BR, BC, BP, and BS are the corresponding number of pixels integrated in the test kernel for each element belonging to T.

3.3 Calibrating the Model

Model calibration is a critical step to simulated the year 1999 using LULC satellite data from 1989, then from 1999 to model the year 2009, and finally from 2009 to simulate the year 2019. The model inferred the most precisely threshold valueswhich stands for the most realistic statistical and geographical result (Kumar et al., 2009), using the LULC of time t1 and the driving parameters to simulate the LULC of time t2. Trial and error were used to find the threshold values for the four factors (TR, TC, TP, and TS) as well as their integrated pixel count values (BR, BC, BP, and BS).In addition, the script kept track of how each component influenced the new integrated pixel creation. After calibration, We used trend lines and plotted threshold values to predict thresholds for the next step in order to determine the magnitude of future accumulation(Tripathy, 2019).

For precision at all levels of the simulation, the PCA (principal component analysis) differencing method was used (Tripathy, 2019), where the distinction between two images was generated by subtracting the cumulative spatially time pixels t2 from the corresponding time pixels t1. From simultaneous satellite and simulated LULC pictures, dichotomous made-up layers were retrieved. The shared built-up area between the photographs was deducted. If there is a change, resulting in non-zero numbers (1 or -1). For an exact percentage computation, the fraction of these non-zero values relative to the total number of pixels received from satellite pictures was examined.4.

4. Results and Discussion

LULC satellite images were generated and processed to estimate land use/land cover and urban expansion trends beetwen 1989 and 2019. The primary elements driving urban growth were then examined in order to calibrate the model and anticipate the built environment's future scope.

4.1Mapping of LULC and Urban Development

From 1989 to 2019, actual multi-temporary satellite data was used to LULC map at 10-year intervals. The data was then utilised to create a LULC1999-2029 simulation. These simulations were linked to the actual LULC satellite During the calibration of the model (1999 to 2019). Between 1989 and 2019, the real built-up area (as measured by satellite) expanded by 28.325 %, from 70.110 to 131.88 km2. Periodic measurements show that the built-up area in 1989 was 70.110 km2 (32.148 % of total area), and that it rose by 9.285 % to 90.35 km2 (41.432 %) in 1999 (Table 3). With an increase of 12.728%, it climbed to 118.117 km2 (54.16 %) in 2009. With a gain of 6.312 %, the built-up area expanded to 131.88 km2 (60.473 %) in 2019. Between 1989 and 2019, the overall variation in the vegetation zone was -5.354 % The vegetation cover covered 39.857 km2 (18.28 %) in 1989, with a fluctuation of -4.713%, rising to 29.579 km2 (13.56 %) in 2009. (1999). It then rose to 40.374 km2 (18.5 %) in 2009, with a difference of 4.950 % The vegetation cover declined to 28.180 km2 in 2019, a decrease of -5.591 % (12.92 %). From 1989 to 2019, the total fluctuation in the category of water qualities was -0.117%. The area protected by water zones increased from 1.083 km2 (0.496 %) in 1989 to 0.629 km2 (0.288 %) in 1999, with a variance of -0.208 %. With a variance of -0.204 %, this area increased to 0.184 km2 (0.084 %) in 2009.

ISSN: 1686-6576 (Printed) | ISSN 2673-0014 (Online) | © Geoinformatics International

Table 3: LULC region data from 1989 to 2019 (satellite-based vs. simulated)

	Type	Built-up Land			VegetationCover			Water Body			Others		
		Area (km²)	%	Δ %	Area (km²)	%	Δ %	Area (km²)	%	Δ %	Area (km²)	%	Δ %
1989	Actual	70,110	32,148	-	39,857	18,28	-	1,083	0,496	-	107,038	49,08	-
1999	Actual	90,359	41,432	9,285	29,579	13,56	4,713	0,629	0,288	-0,208	97,521	44,72	-4,364
	Simulated	97,811	44,849	12,702	28,980	13,29	4,988	0,548	0,251	-0,245	90,749	41,61	-7,469
2009	Actual	118,117	54,160	12,728	40,374	18,51	4,950	0,184	0,084	-0,204	59,414	27,24	17,474
	Simulated	120,344	55,182	10,332	39,959	18,32	5,034	0,174	0,080	-0,172	57,611	26,42	15,195
2019	Actual	131,883	60,473	6,312	28,180	12,92	5,591	0,827	0,379	0,295	57,198	26,23	-1,016
	Simulated	134,867	61,841	6,659	27,934	12,81	5,514	0,640	0,293	0,214	54,647	25,06	-1,359
1989-2019	Actual	-	-	28,325	-	-	5,354	-	-	-0,117	-	-	22,853
	Simulated	-	-	29,693	-	-	5,467	-	-	-0,203	-	-	24,023

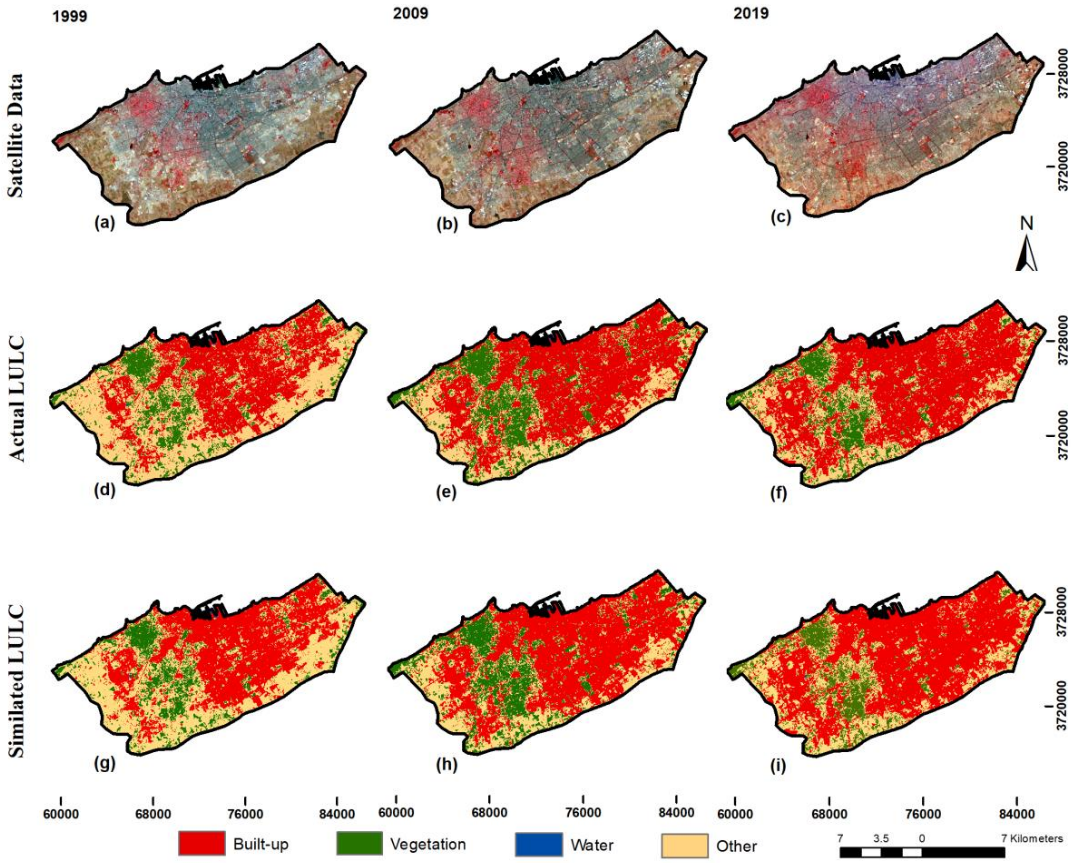

Figure 3: Satellite Data for 1999, 2009 and 2019 (a,b,c), Real LULC (d to f), and Simulated LULC (g to f)

The overall area of water zones climbed to 0.827 km2 in 2019, an increase of 0.295% (0.379 %). The average reduction in the class “other” was -22.853% the class other occupied a total area of 107.038 km2 (49.08%) in 1989, but this reduced to 97.521 km2 (44.72%) in 1999, a difference of -4.364 %. The area of the class “other” declined from 59.414 km2 (27.24%) in 2009 to 57.198 km2 (26.23 %) in 2019, a difference of -1.016 %. From 1989 to 2019, our research shows the impact of urban sprawl on different LULC categories.

Casablanca's central region had the most developed land, according to LULC's spatio-temporal mapping. Due to the availability of suitable sites and the acceptance of the new development plan, the building was later extended to the south and southwest, resulting in a population growth.Unbuilt elements are essential components of built environments because they establish the fundamental dynamics between man and nature (Figure 3).

ISSN: 1686-6576 (Printed) | ISSN 2673-0014 (Online) | © Geoinformatics International

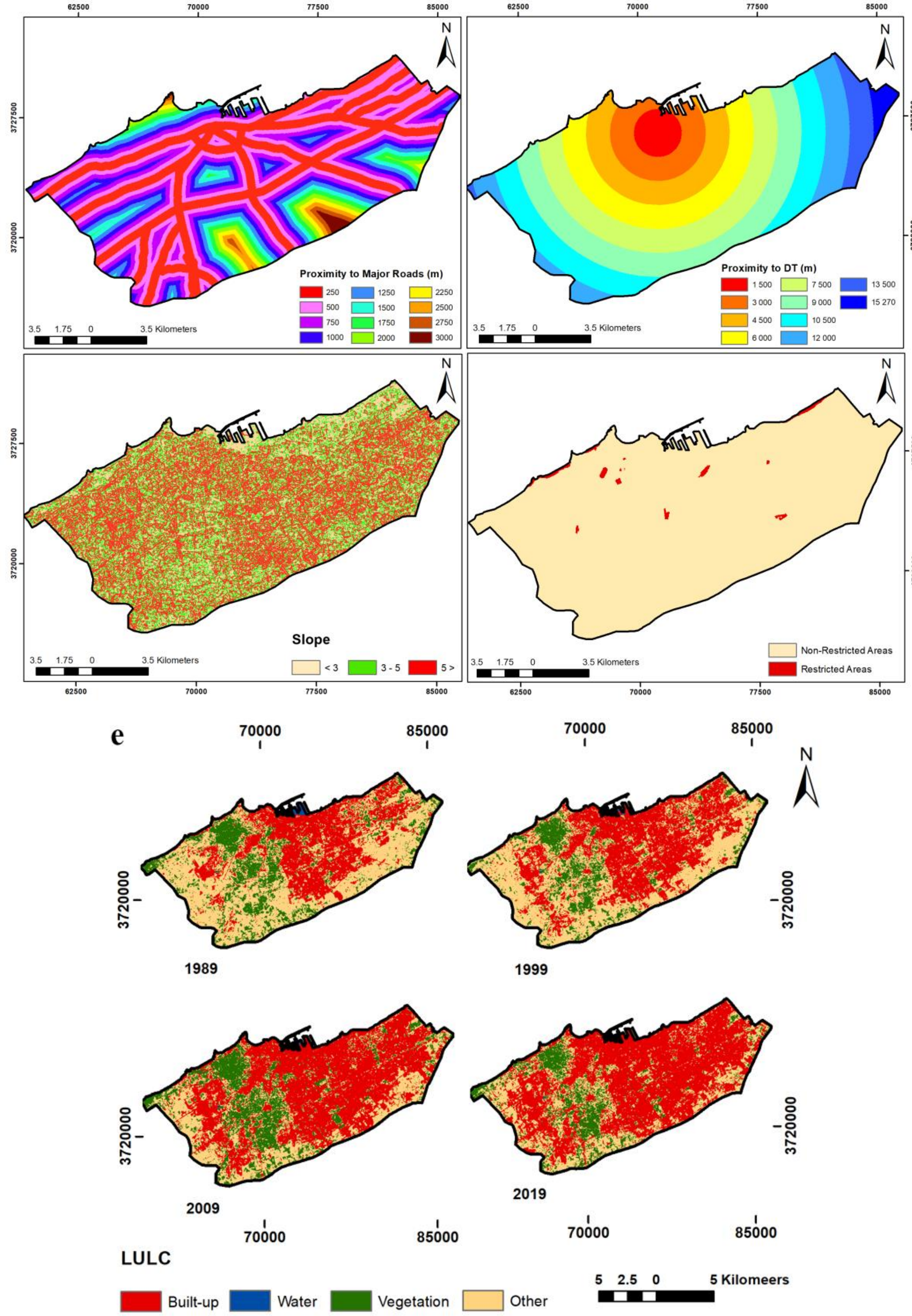

Figure 4: The most important aspects in urban expansion are (a) closeness to mainroadways , (b) proximity to the city center, (c) a slope map based on a digital elevation model (DEM), (d) restricted regions, and (e) temporal satellite-based LULC categorised photos of Casablanca from 1989 to 2019

4.2Urban Growth Contributing Factor

4.2.1 LULC

Different types of LULC Land Use/Land Cover are converted into built-up area in various forms. The class “other” was given a better ranking in this regard, followed by vegetation. In the modeling, constructed land was envisioned as a non-transformable class.

4.2.2 Proximity to major roadways

The density of roads is higher in the city's center and south, while it is lower in the northwest and southwest. The majority of suburban regions have a low road density (Figure 4a).

4.2.3 Slope

According to the investigation, the relief varies between 0 and 197 metres above Casablanca's mean sea level (NGM). The majority of the territory in Casablanca has a slope of less than 5 degrees, but there are a few spots with slopes greater than 5 degrees (See Figure 4c). The slope of the land is one component that has a significant impact on construction growth. Low landforms and moderate slopes provide a more firm foundation for buildings, but high landforms and steep slopes create more runoff, making the terrain less suitable for development. This may explain why low-slope locations have been chosen for development.

4.2.4 Density of population

In the early phases, the population density chart in Casablanca shows a surge in the East zone> 450,000 persons (1994-2014) (Figure 5). Between 1994 and 2004, population density in the southern and western regions changed. The High Commission for Planning and Demographic Forecasting of Morocco's population density maps (2024) demonstra a rise in population density in the East and West.

4.3Modeling of Urban Development Using CA

For various years, the simulated construction was equivalent to the actual building, as illustrated in Figure 6. Built-up land is expected to grow from 131.883 km2 in 2019 to 148.995 km2 in 2029 (12.97 percent built expansion) in the city's west, south and east (Table 5), with densification and distributed development largely in the city's west and south. The area covered by vegetation will rise from 28.180 km2 in 2019 to 26.571 km2 in 2029 (-5.707 percent variation). The 'other' group's area is anticipated to decline, falling from 57.198 km2 in 2019 to 41.85 km2 in 2029(Figure 7).

4.4 Discussion

Most of the anticipated growth takes place inland and along the coast. All anticipated expansion zones, however, are situated at the present limits of the city. Such a pattern is anticipated given that Casablanca is an older, heavily built city with little available undeveloped area inside the city's present boundaries.

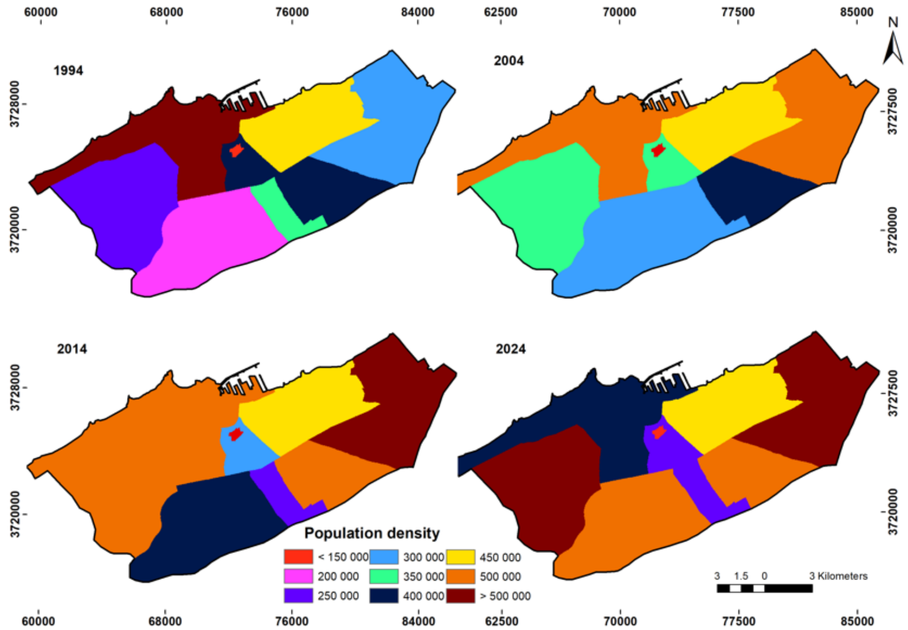

Figure 5: Population density maps of Casablanca for the years 1994, 2004, 2014, and 2024

ISSN: 1686-6576 (Printed) | ISSN 2673-0014 (Online) | © Geoinformatics International

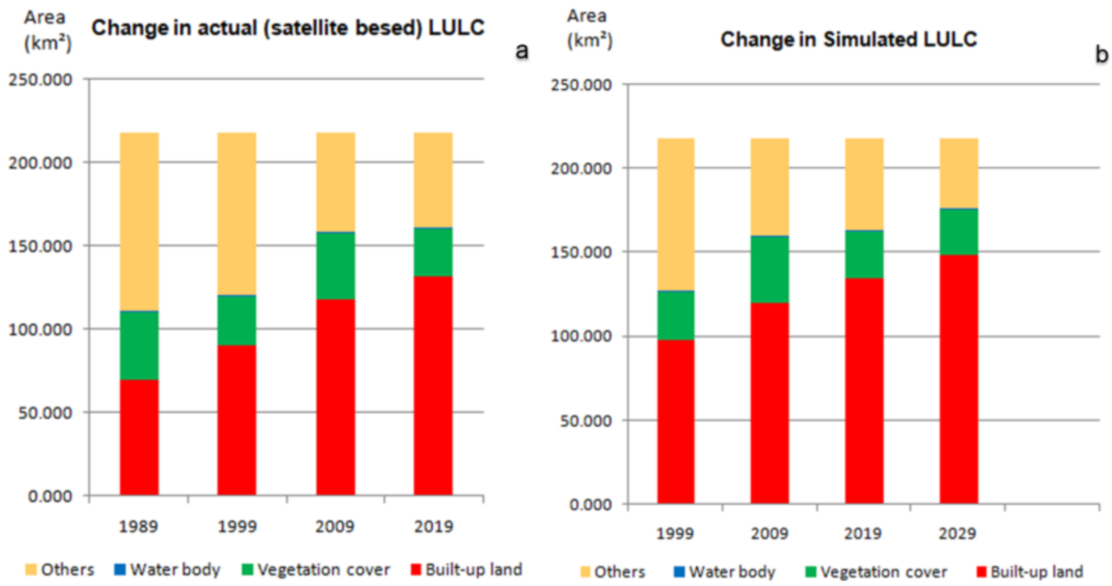

Figure 6: (a) The real and (b)simulated changes in LULC

Table 4: Satellite-based and simulated photographs of built-up areas show statistical diversity

Variables	**Built-up areas in km²**		
	1999	**2009**	**2019**
Actual (Km²)	90,359	118,117	131,883
Simulated (Km²)	97,811	120,344	134,867
Spatial accuracy	89 %	87 %	90 %

Table 5: Statistics of différent classes for 2019 and predicted 2029 with percentage change

	2019 (Km²)	**2029 (Km²)**	**% Change 2019-2029**
Built-up	131,883	148,995	12,974
Vegetation	28,180	26,5716	-5,707
Water	0,827	0,6714	-18,824
Other	57,198	41,85	-26,832

Second, the distribution of the anticipated peripheral growth inside the city is essentially uniform. This anticipated uniform peripheral growth may be explained by the city's rapid population growth rates as well as the substantial labor migration from the nearby farms (Mallouk et al., 2019). The city's current boundaries are where the population expansion from within the city and the migration from the nearby farms naturally collide, accelerating the growth along these boundaries. Consider the city of Ain Harrouda, which is located in a coastal region between Casablanca and Mohemmedia. The east side of Casablanca is expected to experience major growth (AinSebaa and Moulay Rachid District). Strong highway connectivity, particularly the A1 and N9 highways, supports these zones. Similar predictions for Mediouna, Bouskoura, and Ain Chock forecast growth along highways R315 and N1, respectively, on the south side.

Table 6: Real and simulated 2019 built-up pixels confusion matrix

		Predicted		Percentage correct	Overall accuracy
		Non-built-up	Built-up		
Actual	Nonbuilt-up	325730	19013	94.48%	
	Built-up	0	146537	100%	96.13%

Table 7: Matrix of transitions (satellite-based between 1989 and 2019)

	Built Up	Vegetation	Water	Others
built up	0,532	0	0	0,468
vegetation	0	0,414	0	-0,414
water	0	0	1,310	-0,310
others	0,577	-0,109	0,010	0,534

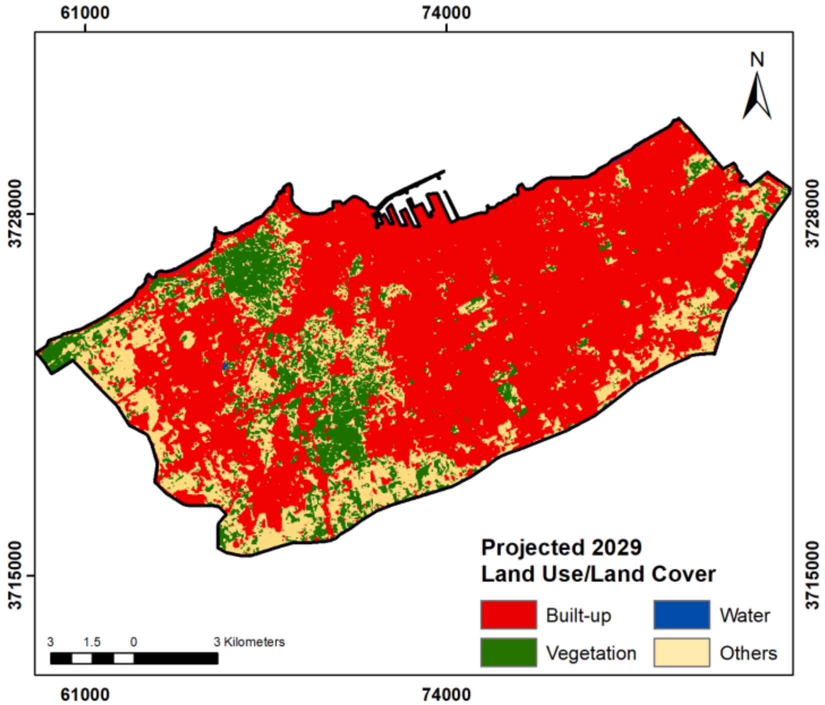

Figure 7: Simulated built-up area growth using a cellular automata (CA) algorithm for 2029

5. Validation of the LULC Simulation

An investigation of the precision indicated a very excellent similarity in both statistics and space similarity (> 87 percent) between the simulated LULC and the real LULC satellite for the given years (1999-2019), Table 4shows the results. The overall precision of the genereted confusion matrix was 96.13 percent (Table 6), and the receiver operating characteristics (ROC) graph's area under the curve (AUC) was 0.94 (Figure 8). The confusion matrix and AUC are exceedingly precise, implying that the modeling is extremely accurate.This is most likely because the calibration was done at regular intervals using an average prediction time (10 years). Table 7 demonstrates that the majority of produced pixels remained in the same class (0.532), with just a minor percentage being changed to a different class (0.468). This could be the result of misclassification due to similar reflectance of elements in recent years compared to prior years, or it could be the result of enhanced satellite data resolution in recent years compared to past years.A similar problem was discovered in several of the "other"classes (0.577). Similarly, in the class "other", some areas have been converted to buildings (0.577) and a tiny number to water class (0.010).Table 8 shows the transition matrix from 2019 to 2029. Pixels from class "other" were used to create pixels for the built class (0.268).

ISSN: 1686-6576 (Printed) | ISSN 2673-0014 (Online) | © Geoinformatics International

Table 8: Matrix of transitions (satellite-based between 2019 and 2029)

	Built Up	Vegetation	Water	Others
built up	0,885	0	0	0,103
vegetation	0	0,943	0	0
water	0	0	0,811	0,000
others	0,268	0	0	0,732

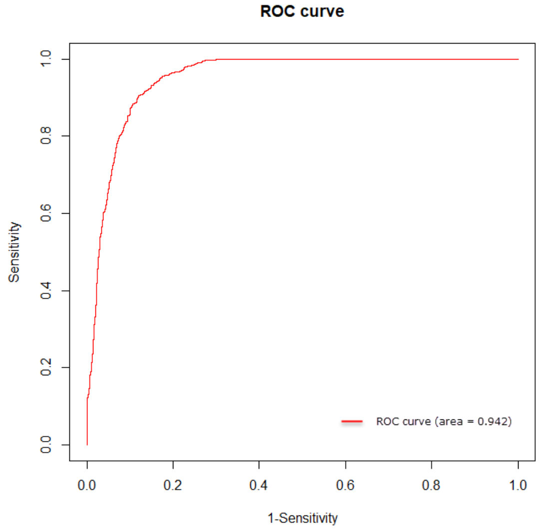

Figure 8: Curve of receiver operating characteristic (ROC) for the real and simulated built-up land during 2019

6. Potential Urban Growth's Impact on Various LULC

The urban growth model based on CA predicted a 17.11 km2 rise in urban areas and a 12.97 percent increase in urban growth rate During the years 2019-2029 (Table 5). Other classes will be impacted: 5.70 km2 of vegetation cover will be lost, 18.82 km2 of water-covered areas will be lost, and 26.83 km2 of other areas will be lost. According to research, Casablanca's urban growth rate would be low between 2019 and 2029.

7. Conclusions

The study uses the CasablancaLULC'sspatio-temporal monitoring (1989-2019) and urban development modeling (1999-2029) to investigate the effect of urban growth on the variety of land use / land cover. Between 1989 and 2019, the real and simulated LULC showed considerable urban development (net expansion of 61,773 km2), leading to a land use change in Casablanca. the remaining classes have been influenced by urbanization: -22.85% vegetation cover (-5.36%) and class of water (-0.117%).

The simulated CA model -based LULC demonstrates that the city is going to from 131.88 to 148.995 km^2 in 2029. LULC's "other" category (loss of 15.348 km2) and the vegetative cover category will be replaced and transformed by urban development between 2019 and 2029. (loss of 1.608 km2). During the years 1989–2019, the transition dynamics in the simulated and satellite LULC were parallel. The assessment of geographic variance was out using the PCA technique between 1999 and 2019 revealed good construction precision. The confusion matrix's overall precision (96.13%) and of the area under Receiver Operating Characteristic (ROC) Curve. (0.94) underlines the high precision of the modeling the study has attempted to simulate and predict the future expansion over time (1999–2029), which the strong impact on changes to built-up areas the initial observation period.This model, which uses remote sensing, GIS, and the CA model to predict future urban evolutionary and spatiotemporal dynamics, is a new technique to dealing with complicated interactions between urbanization and a many of spatial factors. This model can aid planners in making decisions, and it can simply be incorporated into other environmental or ecological approaches to examine the environmental impacts of urbanization. This methodology can be adapted to other cities undergoing fast urbanization.We can therefore draw the conclusion that our initial theory on the use of the CA model in the Grand Casablanca area is confirmed.

Additionally, cellular automata models in conjunction with remote sensing and geographic information systems are appropriate methods to statistically and geographically assess existing and future urban expansion. To cut down on the time needed to process and clean the input data for the model, it is helpful to suggest using very high resolution satellite images.Additionally, it would be very important to combine the methodology proposed in this study with a different model that allows the integration of other parametrs.

References

Babakan, A. S. and Taleai, M., 2015, Impacts of transport Development on Residence Choice of Renter Households: An Agent-Based Evaluation. *Habitat International*, Vol. 49, 275-285.

Batty, M. and Xie, Y., 1994., From Cells to Cities. *Environment and Planning B: Planning and Design*, Vol. 21(7), S31-S48.

Batty, M., Xie, Y. and Sun, Z., 1999, Modeling Urban Dynamics through GIS-based Cellular Automata. *Computers, Environment and Urban Systems*, Vol. 23(3), 205-233.

Chaudhuri, G. and Clarke, K., 2013, The SLEUTH Land Use Change Model: A Review. *Environmental Resources Research*, Vol. 1(1), 88-105. https://doi.org/10.22069/ijerr.2013.1688.

Clarke, K. C., Hoppen, S. and Gaydos, L., 1997, A Self-Modifying Cellular Automaton Model of Historical Urbanization in the San Francisco Bay Area. *Environment and Planning B: Planning and Design*, Vol. 24 (2), 247-261. https://doi.org/10.1068/b240247.

He, C., Okada, N., Zhang, Q., Shi, P. and Zhang, J., 2006, Modeling Urban Expansion Scenarios by Coupling Cellular Automata Model and System Dynamic Model in Beijing, China. *Applied Geography*, Vol. 26(3-4), 323-345.

He, C., Shi, P., Chen, J., Li, X., Pan, Y., Li, J., Li, Y. and Li, J., 2005, Developing Land Use Scenario Dynamics Model by the Integration of System Dynamics Model and Cellular Automata Model. *Science in China Series D: Earth Sciences*, Vol. 48(11), 1979-1989.

Hosseinali, F., Alesheikh, A. A. and Nourian, F., 2013, Agent-based Modeling of Urban Land-Use Development, Case Study: Simulating Future Scenarios of Qazvin City. *Cities*, Vol. 31, 105-113.

Hu, Z. and Lo, C. P., 2007, Modeling Urban Growth in Atlanta Using Logistic Regression. *Computers, Environment and Urban Systems*, Vol. 31(6), 667-688.

Jaad, A. and Abdelghany, K., 2021, The Story of Five MENA Cities: Urban Growth Prediction Modeling Using Remote Sensing and Video Analytics. *Cities,* Vol. 118, https://doi.org/10.1016/j.cities.2021.103393

Kumar, U., Mukhopadhyay, C., Ramachandra, T. V., 2009, Cellular Automata and Genetic Algorithms Based Urban Growth Visualization for Appropriate Land Use Policies. *The Fourth Annual International Conference on Public Policy and Management, Centre for Public Policy, Indian Institute of Management (IIMB)*. 1-27, http://wgbis.ces.iisc.ac.in/energy/paper/-iimb_cellular_automata/cellular_automata.pdf.

Li, X. and Yeh, A. G. O., 2002, Neural-Network-Based Cellular Automata for Simulating Multiple Land UseChanges Using GIS. *International Journal of Geographical Information Science*, Vol. 16(4), 323-343.

Li, X. and Yeh, A. G. O., 2004, Data Mining of Cellular Automata's Transition Rules. *International Journal of Geographical Information Science*, Vol. 18 (8), 723-744.

Li, D., Li, X., Liu, X. P., Chen, Y. M., Li, S. Y., Liu, K., Qiao, J. G., Zheng, Y. Z., Zhang, Y. H. and Lao, C. H., 2012, GPU-CA Model for Large-Scale Land-Use Change Simulation. *Chinese Science Bulletin*, Vol. 57(19), 2442-2452.

Liao, F. H. F. and Dennis Wei, Y. H., 2014, Modeling Determinants of Urban Growth in Dongguan, China: A Spatial Logistic Approach. *Stochastic Environmental Research and Risk Assessment*, Vol. 28 (4), 801-816.

Liu, X., Ma, L., Li, X., Ai, B., Li, S. and He, Z., 2014, Simulating Urban Growth by Integrating Landscape Expansion Index (LEI) and Cellular Automata. *International Journal of Geographical Information Science*, Vol. 28(1), 148-163.

Liu, X., Ma, L., Li, X., Ai, B., Li, S. and He, Z., 2014, Simulating Urban Growth by Integrating Landscape Expansion Index (LEI) and Cellular Automata. *International Journal of Geographical Information Science*, Vol. 28(1), 148-163.

Mallouk, A., Elhadrachi, H., Malaainine, M. and Rhinane, H., 2019, Using the SLEUTH Urban Growth Model Coupled with aGis to Simulate and Predict the Future Urban Expansion of Casablanca Region, Morocco. *ISPRS - International Archives of the Photogrammetry, Remote Sensing and Spatial Information Sciences* XLII-4/W12 (février): 139-145. https://doi.org/10.5194/isprs-archives-XLII-4-W12-139-2019.

Michalak, W. Z., 1993, GIS in Land Use Change Analysis: Integration of Remotely Sensed Data into GIS. *Applied Geography*, Vol. 13(1), 28-44.

Mohammady, S. and Delavar, M. R., 2016, Urban Sprawl Assessment and Modeling Using Landsat Images and GIS. *Modeling Earth Systems and Environment*. Vol. 2(3), 1-14, DOI:10.1007/s40-808-016-0209-4.

Mom, K. and Ongsomwang, S., 2016, Urban Growth Modeling of Phnom Penh, Cambodia Using Sattelite Imageries and a Logistic Regression Model. *Suranaree Journal of Science & Technology*, Vol. 23(4), 1-20

Mustafa, A., Cools, M., Saadi, I. and Teller, J., 2017, Coupling Agent-Based, Cellular Automata and Logistic Regression into a Hybrid Urban Expansion Model (HUEM). *Land Use Policy*, Vol. 69, 529-540, https://doi.org/10.1016/j.land-usepol.2017.10.009.

Navid, D.,1989, The International Law of Migratory Species: the Ramsar Convention. *Nat. Resources J.*, Vol. 29(4), 1001-1016.

Pijanowski, B. C., Gage, S. H., Long, D. T. and Cooper, W. C., 2000, A Land Transformation Model: Integrating Policy, Socioeconomics and Environmental Drivers Using a Geographic Information System. *Landscape Ecology: A Top Down Approach*, 183-198.

Pijanowski, B. C., Brown, D. G., Shellito, B. A. and Manik, G. A., 2002, Using Neural Networks and GIS to Forecast Land Use Changes: A Land Transformation Model. *Computers, Environment and Urban Systems*. Vol. 26(6), 553-575. https://doi.org/10.1016/S0198-9715(01)00015-1.

Pourebrahim, N., Sultana, S., Thill, S. C. and Mohanty, S., 2018, Enhancing Trip Distribution Prediction with Twitter Data: Comparison of Neural Network and Gravity Models. *Proceedings of the 2nd ACM SIGSPATIAL International Workshop on AI for Geographic Knowledge Discovery*, 5-8.

Saadani, S., Laajaj, R., Maanan, M., Rhinane, H. and Aaroud, A., 2020, Simulating Spatial–Temporal Urban Growth of a Moroccan Metropolitan Using CA–Markov Model. *Spatial Information Research*, Vol. 28(5), 609-621.

Seto, K. C., 2011, Exploring the Dynamics of Migration to Mega-Delta Cities in Asia and Africa: Contemporary Drivers And Future Scenarios. *Global Environmental Change*, Vol. 21, S94- S107.

Shi, W. and Pang, M. Y. C., 2000, Development of Voronoi-Based Cellular Automata-An Integrated Dynamic Model for Geographical Information Systems. *International Journal of Geographical Information Science*, Vol. 14(5), 455-74.

Tahami, H., Basiri, A., Moore, T., Park, J. andBonenberg, L., 2018., Virtual Spatial Diversity Antenna for GNSS Based Mobile Positioning in the Harsh Environments. *Proceedings of the 31st International Technical Meeting of the Satellite Division of the Institute of Navigation (ION GNSS+ 2018)*, 3186-3198.

Tayyebi, A. and Pijanowski, B. P.,2014, Modeling Multiple Land Use Changes Using ANN, CART and MARS: Comparing Tradeoffs in Goodness of Fit and Explanatory Power of Data Mining Tools. *International Journal of Applied Earth Observation and Geoinformation*, Vol. 28, 102-116.

Tayyebi, A., Pijanowski, C. B. and Tayyebi, A. H., 2011, An Urban Growth Boundary Model Using NeuralNetworks, GIS and Radial Parameterization: An Application to Tehran, Iran.*Landscape and Urban Planning*, Vol. 100(1-2), 35-44.

Tian, G., Ma, B., Xu, X., Liu, X., Xu, L., Liu, X., Xiao, L. and Kong, L., 2016, Simulation of Urban Expansion and Encroachment Using Cellular Automata and Multi-Agent System Model-A Case Study of Tianjin Metropolitan Region, China . *Ecological Indicators*. Vol. 70, 439-450.

Tobler, W. R., 1970, A Computer Movie Simulating Urban Growth in the Detroit Region. *Economic Geography*, Vol. 46 (sup1), 234-240.

Tripathy, P., 2019, Monitoring and Modelling Spatio-Temporal Urban Growth of Delhi Using Cellular Automata and Geoinformatics. *Cities*, Vol. 12, 52-63.

White, R. and Engelen, G., 2000, High-resolution Integrated Modelling of the Spatial Dynamics of Urban and Regional Systems. *Computers, Environment and Urban Systems*, Vol. 24(5), 383-400.

Wu, F., 2002, Calibration of Stochastic Cellular Automata: The Application to Rural-Urban Land Conversions. *International Journal of Geographical Information Science*, Vol. 16(8), 795-818.

Wu, F. and Martin, D., 2002, Urban Expansion Simulation of Southeast England Using Population SurfaceModelling and Cellular Automata. *Environment and Planning A*, Vol. 34(10), 1855-1876.

Zhang, Y., Li, X., Liu, X. and Qiao, J., 2011, The CA Model Based on Data Assimilation. *Journal of Remote Sensing*, Vol. 15(3), 475-491.